nature photonics

SUPPLEMENTARY INFORMATION

https://doi.org/10.1038/s41566-018-0241-1

In the format provided by the authors and unedited.

Terahertz dynamics of electron–vibron coupling in single molecules with tunable electrostatic potential

Shaoqing Du[1]*, Kenji Yoshida[1], Ya Zhang[1,4], Ikutaro Hamada[2,5] and Kazuhiko Hirakawa[1,3]*

[1]Institute of Industrial Science, University of Tokyo, Meguro-ku, Tokyo, Japan. [2]Center for Green Research on Energy and Environmental Materials, National Institute for Materials Science, Tsukuba, Japan. [3]Institute for Nano Quantum Information Electronics, University of Tokyo, Meguro-ku, Tokyo, Japan. [4]Present address: Institute of Engineering, Tokyo University of Agriculture and Technology, Koganei, Tokyo, Japan. [5]Present address: Department of Precision Science and Technology, Osaka University, Suita, Osaka, Japan. *e-mail: sqdu@iis.u-tokyo.ac.jp; hirakawa@iis.u-tokyo.ac.jp

1. Density functional theory (DFT) calculation of the van der Waals potential

All the DFT calculations were performed by employing the self-consistent implementation[1-3] of the van der Waals density functional[4-6] as implemented in the STATE[7] code. The electron-ion interactions were described by using the ultrasoft pseudopotentials[8]. The surface was modeled by a five-layer-thick Au(111) slab with a ($2\sqrt{3}\times2\sqrt{3}$) periodicity, separated by the vacuum equivalent to fifteen monolayers. The slab was constructed by using the theoretical lattice constant (0.4116 nm). The wave functions and augmentation charge density were expanded in terms of a plane-wave basis set with the cutoff energies of 36 and 400 Ry, respectively. The surface Brillouin zone was sampled with the Γ-centered 2×2 *k*-point set. The adsorbate was put on one side of the slab, and the spurious electrostatic interaction between the neighboring slabs was eliminated by using the effective screening medium method.[9,10] C_{60} was adsorbed on the fcc hollow site with its hexagon faced to the surface. The negatively charged C_{60} was modeled using a method proposed in Ref. 11. The center-of-mass vibrational energy of C_{60} (C_{60}^{-}) on the gold substrate was obtained by solving the one-dimensional Schrödinger equation based on the interaction energy curve for C_{60} (C_{60}^{-}) and Au(111).

2. Statistics for the fabrication of C_{60} & $Ce@C_{82}$ single molecule transistors

By using the feedback-controlled electromigration, we can create sub-nm gap electrodes very reproducibly. The yield of capturing a single molecule in the nanogap region is typically ~15 %. However, the yield of the samples that show the gate field effect is low (~ 6%). Even when the sample exhibited a rather clean Coulomb stability diagram, but if the junction conductance was too low (weak coupling), we could not observe THz photocurrent. Because of these reasons, the number of samples that exhibited THz signals was very few.

Table S1 shows the statistics of the samples we measured in the experiments. For single C_{60} molecule, the yield of obtaining THz spectra is ~2%. For single $Ce@C_{82}$ molecule, it is even lower (~1%).

Table S1 Statistics of the measured C_{60} & $Ce@C_{82}$ single molecule transistors

Sample	C_{60}	$Ce@C_{82}$
Total number of fabricated junctions	~200	~100
Nonlinear I-V curve	~35	~10
Gate field effect	15	3
- Weak coupling ($G \leq 5$ μS)	10	1
- Strong coupling ($G \geq 5$ μS)	5	2
Obtain THz spectrum	4	1

2.1. THz spectrum of a C_{60} single molecule transistor

To obtain reliable THz data on single molecule transistor (SMT) structures, we have empirically found that the following three conditions are important;

1) SMT samples need to be stable during long scans at operating bias conditions. Since it takes a few tens of minutes to measure an interferogram of the THz photocurrent, the system need to be stable against fluctuations due mainly to charge trapping/detrapping.

2) The Coulomb stability diagrams of SMTs should be clean. At least, the crossing lines for the ground state tunneling should be clearly visible.

3) The tunneling conductance needs to be greater than ~10 μS to observe measurable THz photocurrent.

Particularly, the condition 1 is very crucial to obtain reliable THz spectra, because interferograms can easily be destroyed by spontaneous jumps in the THz photocurrent.

To back up the argument developed in the main body of this paper, we fabricated more single molecule transistor samples. Fig. S1 shows the result of another single C_{60} molecule transistor. As we see in Fig. 2e, two split peaks are observed around 2 meV and a broad peak around 4 meV is seen, supporting the reproducibility of the data shown in Fig. 2.

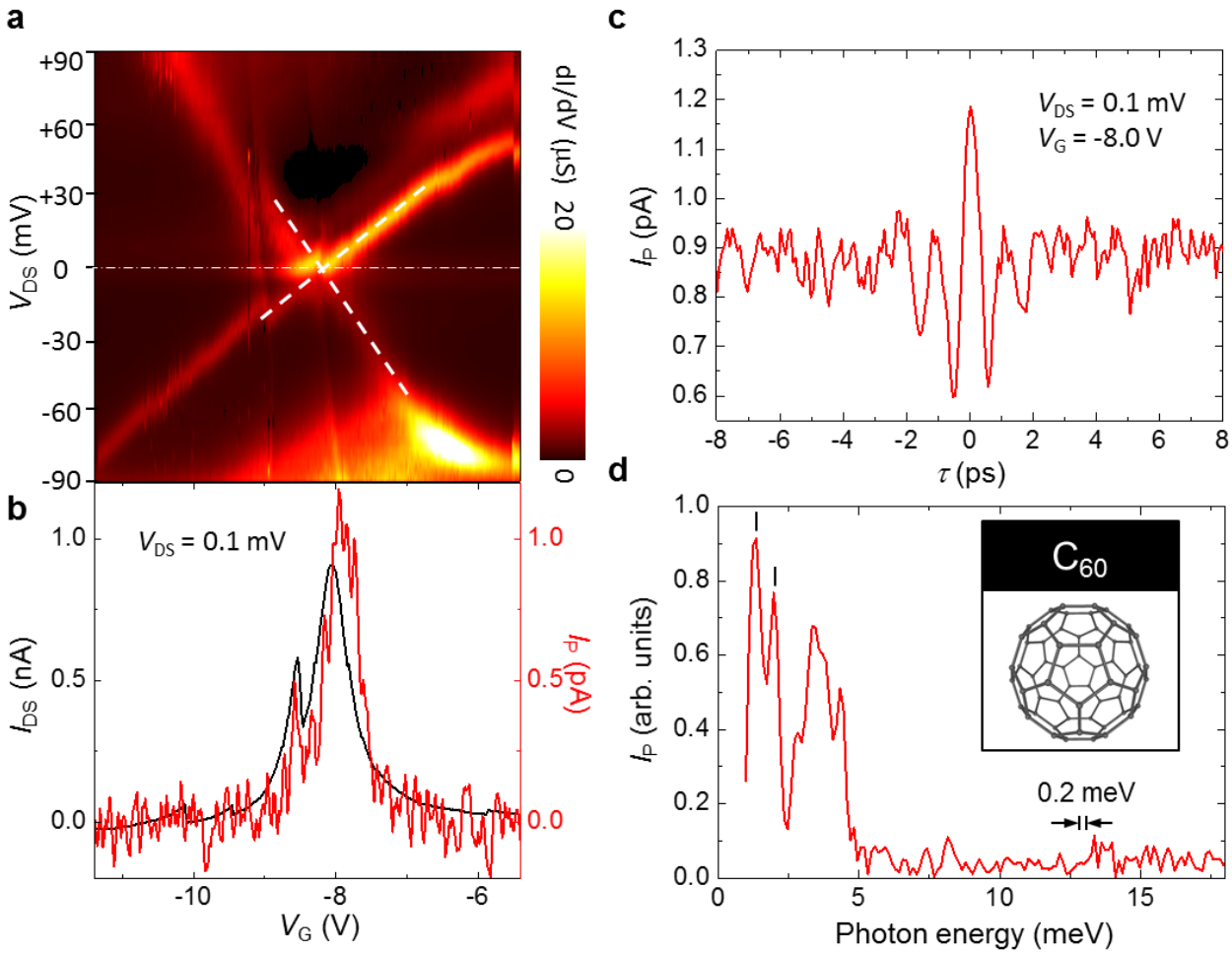

Fig. S1 Transport and THz data measured on another C_{60} single molecule transistor (SMT). **a**. Coulomb stability diagram of a C_{60} SMT. White dashed lines are eyeguides for the boundaries of the Coulomb diamonds. **b**. The single electron tunneling current I_{DS} in the dark (black curve) and the THz-induced photocurrent I_P (red curve) as a function of V_G measured at V_{DS} = 0.1 mV. The structure at V_G = -8.7 V is due to charge trapping/detrapping and not essential. **c**. Quasi-autocorrelation trace (interferogram) of the THz induced photocurrent measured at the peak of the photocurrent (V_G = -8.0 V, V_{DS} = 0.1 mV). The quasi-autocorrelation trace was obtained by averaging data for 12 scans. **d**. Fourier spectrum of the interferogram shown in **c**. The spectrum exhibits sharp split peaks at ~2 meV and a broad peak at ~4 meV.

2.2. THz spectroscopy of a Ce@C_{82} single molecule transistor

We measured a THz spectrum of a Ce@C_{82} single molecule transistor (SMT). Figure S2a shows the interferogram of the THz induced photocurrent. Figure S2b shows its Fourier spectrum, which is the same as Fig. 2f in the main body of the present paper. Vibrational peaks with a sharp splitting appear around 2 meV.

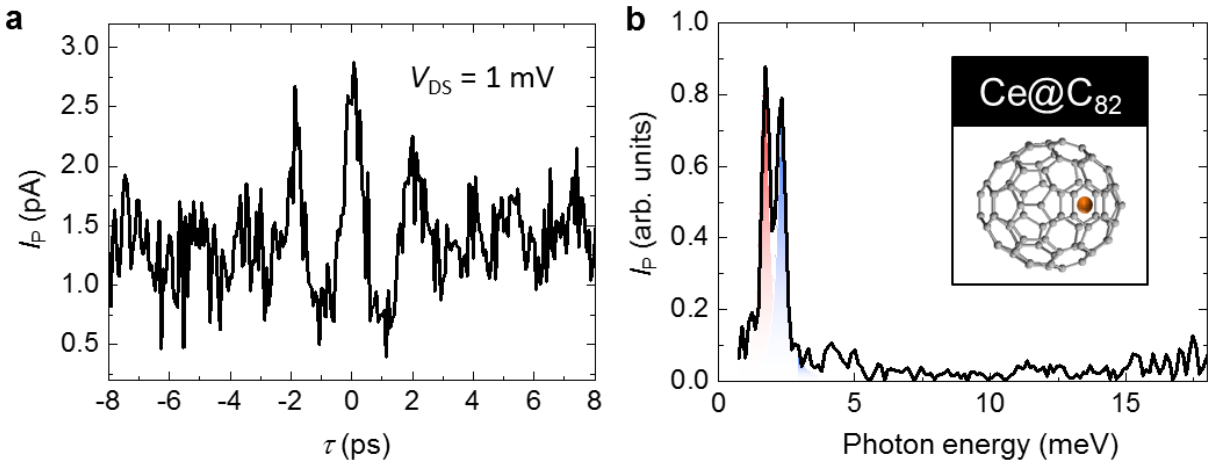

Fig. S2 THz data measured on a Ce@C_{82} SMT. **a**. The interferogram of the THz-induced photocurrent measured on a Ce@C_{82} SMT. **b**. Fourier spectrum of **a**.

3. Franck-Condon principle for vibron-assisted transition

The Franck-Condon principle predicts that the transition probability between the N-electron vibrational state and the (N+1)-electron vibrational state is proportional to the square of the overlap integral of the vibrational wave functions of the initial state Ψ_i and the final state Ψ_f, $|\langle\Psi_f|\Psi_i\rangle|^2$. The displacement in the center-of-mass position of the molecule for the N- and (N+1)-states, δ, modulates $|\langle\Psi_f|\Psi_i\rangle|^2$.

Figure S3b shows the calculated $|\langle\Psi_f|\Psi_i\rangle|^2$ as a function of g, which is defined as the ratio between the displacement (δ) and the quantum mechanical position uncertainty (x_0), $g = \delta/x_0$. The height ratio between P1 (1-vibron process) and P2 (2-vibron process) for the C_{60} single molecule transistor sample shown in Fig. 2e and Fig. S3a is ~3.7. This value corresponds to g = 1.5. This g is consistent with a value for single C_{60} molecules reported previously.[12,13] If we use g ~ 1.5, P3/P1 is expected to be ~0.05, which means P3 (3-vibron process) is very small, compared with P1. Indeed, the 3-vibron peak is not visible in Fig. S3a.

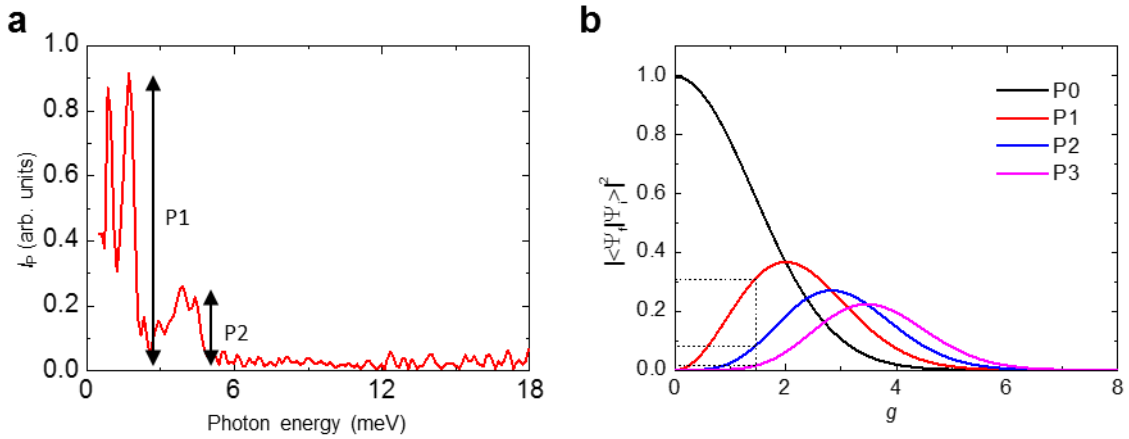

Fig. S3 Vibron-assisted transitions and the Franck-Condon principle. **a**. THz photocurrent spectrum measured on a C_{60} single molecule transistor (replotted from Fig. 2e of the main body of this paper). **b**. Calculated $|\langle\Psi_f|\Psi_i\rangle|^2$ as a function of g. In the present C_{60} SMT sample, g was estimated to be ~1.5.

4. Corresponding figures in Methods

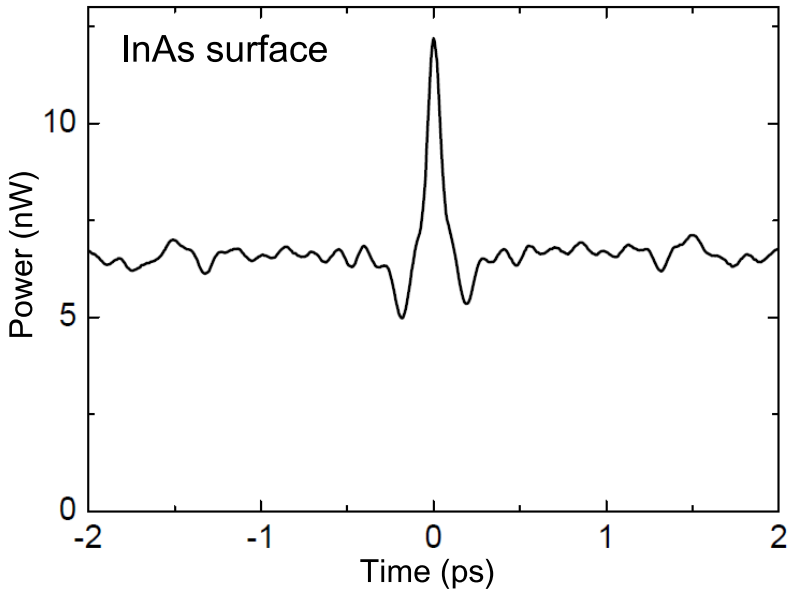

Fig. S4 | Quasi-autocorrelation trace (interferogram) of the THz radiation generated from an InAs surface measured by using a broadband Si bolometer.

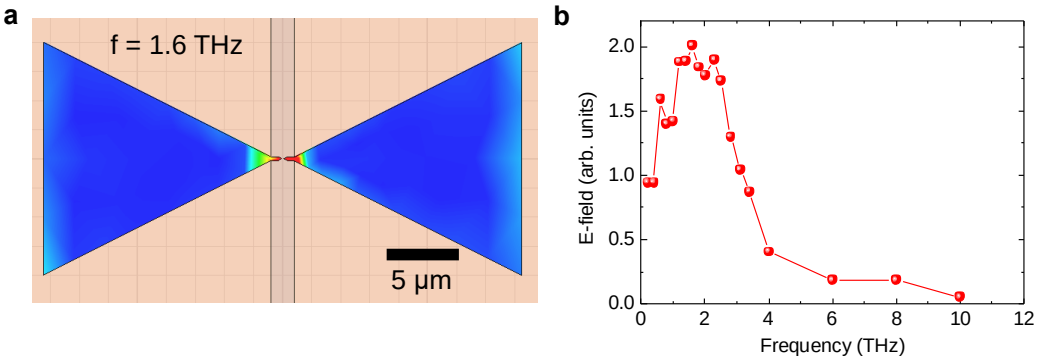

Fig. S5 | **a.** Top view of the source/drain electrodes used in the present work. The electric field distribution at 1.6 THz is plotted in a color code. As seen in the figure, the terahertz field is localized in the gap region. **b.** Spectrum of the THz field strength in the nanogap region. The antenna has a broad resonance around 2 THz.

References

1 Román-Pérez, G. & Soler, J. M. Efficient Implementation of a van der Waals Density Functional: Application to Double-Wall Carbon Nanotubes. *Physical Review Letters* **103**, 096102 (2009).

2 Wu, J. & Gygi, F. A simplified implementation of van der Waals density functionals for first-principles molecular dynamics applications. *The Journal of Chemical Physics* **136**, 224107 (2012).

3 Hamamoto, Y., Hamada, I., Inagaki, K. & Morikawa, Y. Self-consistent van der Waals density functional study of benzene adsorption on Si(100). *Physical Review B* **93**, 245440 (2016).

4 Dion, M., Rydberg, H., Schröder, E., Langreth, D. C. & Lundqvist, B. I. Van der Waals Density Functional for General Geometries. *Physical Review Letters* **92**, 246401 (2004).

5 Lee, K., Murray, É. D., Kong, L., Lundqvist, B. I. & Langreth, D. C. Higher-accuracy van der Waals density functional. *Physical Review B* **82**, 081101 (2010).

6 Hamada, I. van der Waals density functional made accurate. *Physical Review B* **89**, 121103 (2014).

7 Morikawa, Y., Ishii, H. & Seki, K. Theoretical study of n-alkane adsorption on metal surfaces. *Physical Review B* **69**, 041403 (2004).

8 Vanderbilt, D. Soft self-consistent pseudopotentials in a generalized eigenvalue formalism. *Physical Review B* **41**, 7892-7895 (1990).

9 Otani, M. & Sugino, O. First-principles calculations of charged surfaces and interfaces: A plane-wave nonrepeated slab approach. *Physical Review B* **73**, 115407 (2006).

10 Hamada, I., Otani, M., Sugino, O. & Morikawa, Y. Green's function method for elimination of the spurious multipole interaction in the surface/interface slab model. *Physical Review B* **80**, 165411 (2009).

11 Hamada, I., Araidai, M. & Tsukada, M. Origin of nanomechanical motion in a single-C_{60} transistor. *Physical Review B* **85**, 121401 (2012).

12 Park, H. *et al.* Nanomechanical oscillations in a single-C_{60} transistor. *Nature* **407**, 57-60

(2000).

13 Park, J. *Electron Transport in Single Molecule Transistors*. Ph. D. thesis, UNIVERSITY OF CALIFORNIA, BERKELEY, (2003).